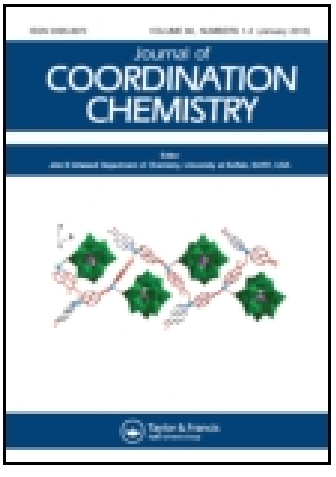

Journal of Coordination Chemistry
Publication details, including instructions for authors and subscription information:
http://www.tandfonline.com/loi/gcoo20

Synthesis, crystal structures, antimicrobial activities, and DFT calculations of two new azido nickel(II) complexes

Behrouz Shaabani[a], Ali Akbar Khandar[a], Michal Dusek[b], Michaela Pojarova[b], Miguel Anxo Maestro[c], Rabindranath Mukherjee[d] & Farzaneh Mahmoudi[a]

[a] Faculty of Chemistry, Department of Inorganic Chemistry, Tabriz University, Tabriz, Iran

[b] Institute of Physics of the ASCR, v.v.i., Prague, Czech Republic

[c] Departamento de Química Fundamental, Universidade da Coruña, Acoruña, Spain

[d] Department of Chemistry, Indian Institute of Technology Kanpur, Kanpur, India

Accepted author version posted online: 30 Jun 2014.Published online: 31 Jul 2014.

To cite this article: Behrouz Shaabani, Ali Akbar Khandar, Michal Dusek, Michaela Pojarova, Miguel Anxo Maestro, Rabindranath Mukherjee & Farzaneh Mahmoudi (2014) Synthesis, crystal structures, antimicrobial activities, and DFT calculations of two new azido nickel(II) complexes, Journal of Coordination Chemistry, 67:12, 2096-2109, DOI: 10.1080/00958972.2014.936859

To link to this article: http://dx.doi.org/10.1080/00958972.2014.936859

Journal of Coordination Chemistry, 2014
Vol. 67, No. 12, 2096–2109, http://dx.doi.org/10.1080/00958972.2014.936859

Synthesis, crystal structures, antimicrobial activities, and DFT calculations of two new azido nickel(II) complexes

BEHROUZ SHAABANI*†, ALI AKBAR KHANDAR†, MICHAL DUSEK‡, MICHAELA POJAROVA‡, MIGUEL ANXO MAESTRO§, RABINDRANATH MUKHERJEE¶ and FARZANEH MAHMOUDI†

†Faculty of Chemistry, Department of Inorganic Chemistry, Tabriz University, Tabriz, Iran
‡Institute of Physics of the ASCR, v.v.i., Prague, Czech Republic
§Departamento de Química Fundamental, Universidade da Coruña, Acoruña, Spain
¶Department of Chemistry, Indian Institute of Technology Kanpur, Kanpur, India

(*Received 30 September 2013; accepted 18 May 2014*)

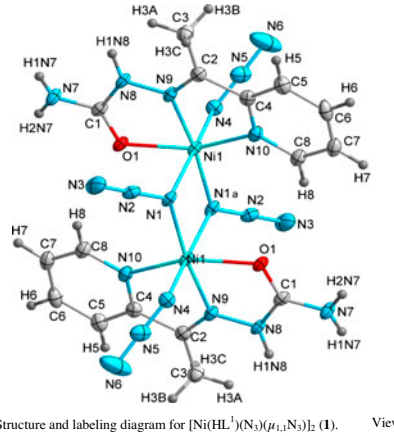

Structure and labeling diagram for $[Ni(HL^1)(N_3)(\mu_{1,1}N_3)]_2$ (**1**).

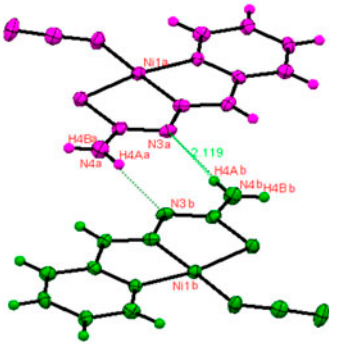

View of the presence of intermolecular H-bonds in $[Ni(L^2)(N_3)]$ (**2**).

Two new complexes, $[Ni(HL^1)(N_3)(\mu_{1,1}N_3)]_2$ (**1**) [HL^1: $NC_5H_4CH_3C{=}NNH$ (C=O) NH_2] and [Ni$(L^2)N_3$] (**2**) [HL^2: $NC_5H_4HC{=}N$ $NH(C{=}S)NH_2$], have been synthesized by reaction of Ni$(OAC)_2{\cdot}4H_2O$ and sodium azide with HL^1 and HL^2 and characterized by elemental analysis, FT-IR, and UV–vis spectral studies. Single-crystal X-ray diffraction reveals that **1** is dinuclear with nickel (II) in an octahedral environment of NNO donors of HL^1, two nitrogens of azide bridges and one nitrogen of terminal azide; **2** is mononuclear containing nickel(II) in a distorted square-planar environment of NNS donors of HL^2 and one terminal azide. The structures of **1** and **2** have been optimized by density functional theory. The results of antimicrobial activities of ligands, **1** and **2** demonstrated that HL^2 and **2** have good antimicrobial activity in contrast with HL^1 and **1**, related to the presence of sulfur donor in HL^2.

Keywords: Semicarbazone and thiosemicarbazone Schiff base; Azido ligand; Nickel(II) complex; X-ray structure; Antimicrobial activity

*Corresponding author. Email: shaabani@tabrizu.ac.ir

1. Introduction

Schiff bases have played a key role as chelating ligands in main group and transition metal coordination chemistry, due to their ease of synthesis and their structural versatility associated with diverse applications [1–5]. Schiff bases are important intermediates for synthesis of some bioactive compounds [6–8]. Semi and thiosemicarbazones are of interest because of their chemistry and potentially beneficial biological, antitumor, antibacterial, antiviral, and antimalarial, activities [9–18]. Semi and thiosemicarbazones belong to the family of Schiff bases which can coordinate to the metal either as neutral or deprotonated ligands through two or three donors [11, 15, 19, 20]. Pseudohalides can form bridging complexes with transition metals where N_3^-, NCS^-, NCO^- coordinate in end-to-end and end-on bridging modes. Azide is a versatile bridging ligand that can link metal ions in μ-$_{1,1}$, μ-$_{1,3}$, μ-$_{1,1,3}$, and other modes, and ferromagnetic and antiferromagnetic interactions can be mediated through different modes [21–30]. We herein report the synthesis, characterization, and X-ray crystal structure of two azido nickel(II) complexes based on semi and thiosemicarbazone Schiff base ligands. Antimicrobial activities of ligands and complexes are reported.

2. Experimental

2.1. *Materials and general methods*

All chemicals and solvents were of reagent grade and used as received from Merck or Fluka. Microanalyses were carried out using a Heraeus CHN–O– Rapid analyzer. Melting points were measured on an Electrothermal 9100 apparatus and are uncorrected. Infrared (IR) spectra were recorded on a FT-IR Spectrometer Bruker Tensor 27 from 4000 to 400 cm^{-1} using KBr pellets. Electronic spectra were recorded on a Shimadzu UV-1650 PC spectrophotometer at 300 K in DMSO.

2.2. *Synthesis of Schiff base ligands*

2.2.1. Methyl 2-pyridyl ketone semicarbazone (HL^1). As seen in scheme 1, HL^1 [11–14] was prepared by condensation of methyl 2-pyridyl ketone with semicarbazide hydrochloride. 0.8 g (7 mM) of semicarbazide hydrochloride was added to a solution of methyl 2-pyridyl ketone (0.85 mL, 7 mM) in 20 mL of methanol in a round-bottom flask under continuous stirring. The mixture was refluxed for 5 h to produce a white suspension. The final reaction mixture was filtered off and the filtrate was kept at room temperature for 10 h. The resulting white precipitate (m.p. 206 °C) was filtered off, washed with methanol, and dried in air. Yield: 1.30 g (5 mM, 80%), Anal. Calcd for $C_8H_{10}N_4O$: C, 44.72; H, 4.66;

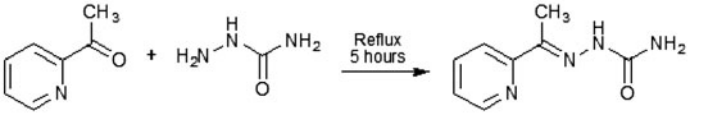

Scheme 1. Reaction for the synthesis of HL^1.

N, 26.08. Found: C, 44.65; H, 4.56; N, 26.08. Characteristic IR absorptions (cm^{-1}): 3431m, $\nu(NH_2)$; 3192m, $\nu(NH)$; 1578s, $\nu(C=N)$; 1105s, $\nu(NN)$; 1685s, $\nu(C=O)$.

2.2.2. Pyridine 2-carbaldehyde thiosemicarbazone (HL^2). The chemical scheme of HL^2 [15, 16] is shown in scheme 2. For synthesis of HL^2, hot ethanolic solution of thiosemicarbazide (0.8 g, 7 mM) and ethanolic solution of pyridine-2-carbaldehyde (0.85 mL, 7 mM) were mixed in the presence of a few drops of concentrated HCl with constant stirring. This mixture was refluxed at 100 °C for 5 h. The reaction mass on cooling gave cream-colored crystals, which were filtered off, washed with ethanol, and dried in air (yield: 1.40 g (87%), m.p. 185 °C). Anal. Calcd for $C_7H_8N_4S$: C, 30.01; H, 2.85; N, 20.01. Found: C, 30.23; H, 2.98; N, 20.32. Characteristic IR absorptions (cm^{-1}): 3424m, $\nu(NH_2)$; 3185m, $\nu(NH)$; 1604s, $\nu(C=N)$; 1112s, $\nu(N–N)$; 844s, 1246s, $\nu(C=S)$.

Caution! Metal azido compounds are potentially explosive. Only a small amount of material should be prepared and should be handled with prudence.

2.3. *Synthesis of complexes*

2.3.1. $[Ni(HL^1)(N_3)(\mu_{1,1}N_3)]_2$ (1). Synthesis of complexes in the form of crystalline material was performed by slow diffusion in an H-shaped tube already described [31–34]. In this method, methyl 2-pyridyl ketone semicarbazone (0.2 mM) was placed in one arm of a branched tube and $Ni(OAC)_2{\cdot}4H_2O$ (0.4 mM) and sodium azide (1.2 mM) in the other. Methanol was carefully added to fill both arms, the tube sealed and the ligand-containing arm immersed in a bath at 60 °C while the other was at ambient temperature. After three days, light-green crystals had deposited in the cooler arm, which were filtered off, washed with acetone and ether, and air dried; yield: 30%, decomposed at 160 °C. Anal. Calcd for $C_{16}H_{20}N_{20}Ni_2O_2$: C, 30.02; H, 3.21; N, 43.73. Found: C, 29.91; H, 3.11; N, 43.62. Characteristic IR absorptions (cm^{-1}): 3412m, $\nu(NH_2)$; 3162m, $\nu(NH)$; 1591s, ν(C=N); 1189s, $\nu(NN)$; 1666s, $\nu(C=O)$; 2061s, $\nu(N_3^-)$.

2.3.2. $[Ni(L^2)(N_3)]$ (2). For synthesis of **2**, 0.2 mM HL, 0.8 mM $Ni(OAC)_2{\cdot}4H_2O$, and 1.2 mM sodium azide in methanol were used. After two days, dark brown crystals (decomposed at 150 °C) had formed which were isolated, filtered off, washed with acetone and diethyl ether, and dried in air. Yield: 0.12 g (30%). Anal. Calcd for $C_7H_7N_7NiS$: C, 30.01; H, 2.50; N, 35.01. Found: C, 30.23; H, 2.76; N, 35.25. Characteristic IR absorptions (cm^{-1}): 3453,3411m, $\nu(NH_2)$; 3189m, $\nu(C=N)$; 1168s, $\nu(N–N)$; 809m, $\nu(C=S)$; 2052s, $\nu(N_3^-)$.

2.4. *X-ray crystallography*

X-ray diffraction data of $[Ni(HL^1)(\mu_{1,1}N_3)(N_3)]_2$ (**1**) were collected at 163 K with a four-circle diffractometer (Gemini of Oxford Diffraction, Ltd) using a sealed X-ray tube

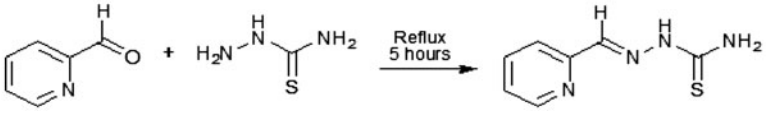

Scheme 2. Reaction for the synthesis of HL^2.

Table 1. Crystal data and structure refinement parameters for **1** and **2**.

	1	**2**
Chemical formula	$C_{16}H_{20}N_{20}Ni_2O_2$	$C_7H_7N_7NiS$
Formula weight	641.90	279.96
Temperature (K)	164 K	100 K
Crystal system	Monoclinic	Monoclinic
Space group	$P2_1/c$	$P2_1/n$
a (Å)	11.1326(3)	3.853(2)
b (Å)	14.2647(3)	16.766(3)
c (Å)	8.4223(2)	15.325(4)
α (°)	90	90
β (°)	106.904(3)	90.108(5)
γ (°)	90	90
Volume (Å^3)	1279.70(6)	990.0(6)
Z	2	4
ρ calculated (g cm^{-3})	1.666	1.878
μ (mm^{-1})	1.531	2.151
T_{min}, T_{max}	0.723, 0.896	0.753, 0.879
θ max (°)	24.710	28.400
Final R indices [$I > 2\sigma(I)$]	0.0209(2001)	0.0462(2002)
Final R indices (all data)	0.0522(2166)	0.1840(2418)
S	1.032	1.146

with MoKα graphite-monochromated radiation (0.7107 Å). The diffracted beam was detected with the Atlas charge-coupled device (CCD) detector. Standard data collection strategy of Crysalis [35] was used for data collection. The crystal structures were solved by SHELXS-97 and refined with SHELXL-97. The materials for publication were prepared by using publCIF.

For $[Ni(L^2)(N_3)]$ (**2**), a suitable single crystal was mounted on a Hampton Research Cryo-Loop with the help of a Stemi 2000 stereomicroscope equipped with Carl Zeiss lenses. Data were collected on a Bruker X8 Kappa APEX II CCD area-detector diffractometer (Mo Kα graphite-monochromated radiation, 0.71073 Å) controlled by the APEX2 software package and equipped with an Oxford Cryosystems Series 700 cryostream monitored remotely using the software interface Cryopad. Images were processed using the software package SAINT, and data were corrected for absorption by the multi-scan semi-empirical method implemented in SADABS. The structures were solved by direct methods implemented in SHELXS-97 and refined from successive full-matrix least-squares cycles on F^2 using SHELXL-97. All non-hydrogen atoms were successfully refined using anisotropic displacement parameters, including those from crystallization solvent molecules (water and n-hexane).

Crystallographic data and details of the data collection and structure refinements of **1** and **2** are listed in table 1.

2.5. *Antimicrobial activity*

The free ligands and metal complexes were screened for antimicrobial activities against the bacteria (*Bacillus subtilis*, *Staphylococcus aureus*, *Escherichia coli*, *Erwinia carotovora*) and fungi (*Candida kefyr*, *Candida krusei*, *Aspergillus niger*) by the disk diffusion method as Gram negative, Gram positive, and fungal organisms, respectively. The culture media (Miller Hinton agar for bacteria, Sabouraud dextrose agar for fungi) were poured into sterile plates and micro-organisms were introduced on the surface of agar plates individually. Blank sterile disks of 6.4 mm diameter were soaked in a known concentration of the test compounds.

Then the soaked disks were implanted on the surface of the plates. A blank disk was soaked in DMSO and implanted as negative control on each plate along with the standard drugs. The plates were incubated at 37 °C (24 h) and 27 °C (48 h) for bacterial and fungal strains, respectively. The MIC for each tested substance was determined by macroscopic observation of microbial growth. It corresponds well with the lowest concentration of the tested substance where microbial growth was clearly inhibited.

2.6. Computational details

The geometry of **1** and **2** has been optimized by using the B3LYP density functional model [36, 37]. In these calculations, we used the 3-21G* basis set for carbon and hydrogen atoms, whereas the 6-31G* basis set was used for nitrogens. For nickel atoms, the LanL2DZ valence and effective core potential functions were used [38, 39]. All DFT calculations were performed using the Gaussian 98 R-A.9 package [40]. X-ray structures were used as input geometries when available.

3. Results and discussion

3.1. *IR spectra*

IR spectral bands of ligands, **1** and **2** are presented in table 2. Formations of Schiff bases have been confirmed by sharp bands at 1578 and 1604 cm^{-1}, respectively, for HL^1 and HL^2, indicating presence of an imine functionality. The band at 1685 cm^{-1} in HL^1 has significant contribution from C=O stretching vibration. A medium band at 3192 cm^{-1} is assigned to ν(N–H) of semicarbazone. Most semicarbazone ligands reveal keto–enol tautomerism in coordination to metal ions, coordinating as neutral or deprotonated forms [11, 13]. In **1**, the presence of a band at 3192 cm^{-1} corresponding to ν(N–H) vibration indicates the HL is coordinated in the keto form. Observation of a band at 1666 cm^{-1} related to C=O stretch supports the keto form [20] of the HL in **1**. HL^2 can exhibit thione–thiol tautomerism since it contains a thioamide–NH–C=S group. The ν(S–H) band at 2565 cm^{-1} is absent in IR spectra of ligand [10]. On coordination of the azomethine nitrogen, the ν(C=N) at 1578 and 1604 cm^{-1} shifts to 1591 and 1638 cm^{-1} for **1** and **2** [20]. The spectra of **1** and **2** exhibit a systematic shift in the position of ν(N–N) bands at 1189 and 1168 cm^{-1} for **1** and **2**, respectively, due to increase in bond strength, which again confirms coordination of azomethine nitrogen to nickel(II) [13, 41, 42]. The band at 844 cm^{-1} for ν(C=S) in HL^2 is shifted to lower wavenumber 809 cm^{-1} for **2**, which indicates coordination via sulfur of thiosemicarbazone

Table 2. IR spectra (cm^{-1}) assignment for ligands, **1,** and **2**.

Compound	ν_{NH2}	ν_{NH}	$\nu_{C=O}$ or $\nu_{C=S}$	$\nu_{C=N}$	ν_{N-N}	ν_{N3}
HL^1	3431	3192	1685	1578	1105	–
HL^2	3424	3185	844	1604	1112	–
1	3412	3162	1666	1591	1189	2061
2	3411	–	809	1638	1168	2052

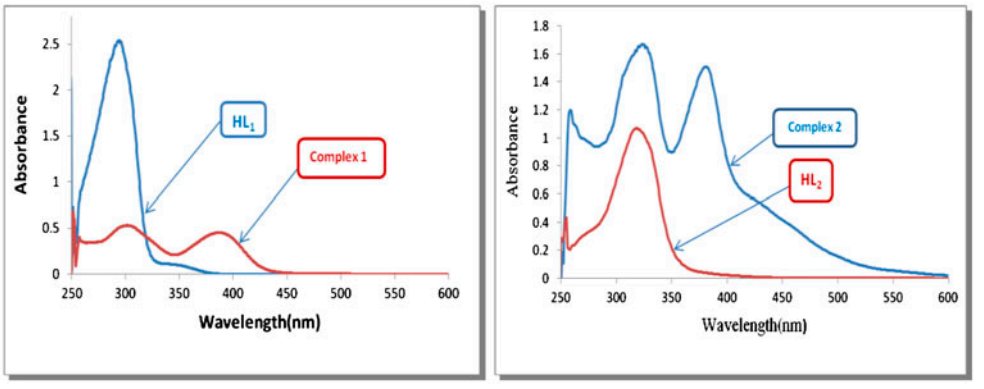

Figure 1. The electronic absorption spectra of HL_1 and **1** (a), HL_2 and **2** (b).

[10]. Complexes **1** and **2** exhibit strong bands at 2061 and 2052 cm^{-1} corresponding to $\nu(N_3)$ of the coordinating azide [24–26, 42, 43].

3.2. *Electronic spectra*

As shown in figure 1, electronic spectra of ligands show absorption maxima at 260 and 295 nm for HL^1 and 255 and 350 nm for HL^2, attributed to intra-ligand $\pi\rightarrow\pi^*$ transitions of the pyridine ring and azomethine group and also a sharp band at 300 nm attributed to $n\rightarrow\pi^*$ transition of imine group for HL^2 [13, 14]. Spectra of the complexes show two different CT bands at 265 and 304 nm for **1** and 260 and 310 nm for **2**. In spectra of the complexes, bands for pyridine and azomethine chromophore shift the $\pi\rightarrow\pi^*$ transition to lower frequencies, indicating that the pyridine and imine nitrogens were involved in coordination [13]. As spectra of the free ligands have no CT bands from 350 to 430 nm, the CT bands at 385 nm for **1** and 380 nm for **2** are associated to $LMCT_{N3}\rightarrow d$ [14, 24, 44, 45]. The presence of intense $\pi\rightarrow\pi^*$ and $LMCT_{N/S/N3\rightarrow d}$ transitions causes the lower energy d–d bands to appear as weak shoulders, bringing about difficulty in assignment of bands.

3.3. *Crystal structures*

3.3.1. Structure of $[Ni(HL^1)(N_3)(\mu_{1,1}N_3)]_2$ (1). A perspective view of **1** is displayed in figure 2. Complex **1** crystallizes in the monoclinic system with space group $P2_1/c$. The crystal data and structure refinement are summarized in table 1. Its structure contains a six-coordinate dinickel complex, in which the two Ni(II) ions are bridged by two azides. The bridging azides are in end-on modes. Each Ni(II) in the dinickel core is further bound by tridentate HL and by a terminal nitrogen of azide. Both nickel centers have distorted octahedral geometry. The apical positions are occupied by two nitrogens; N1 from the azide bridge in EO mode [Ni1–N1 is 2.1288(14) Å] and N4 from the terminal azido [Ni1–N4 is 2.0695(14) Å] with N1–Ni1–N4 angle of 169.56(6)° (for more information about the bond lengths and angles see table 3). The equatorial plane is formed by two nitrogens and one oxygen from chelating HL (N9, N10 and O1) and one nitrogen from the other azide bridge in EO mode (N1). The average Ni–N bond length in the basal plane is 2.036 Å.

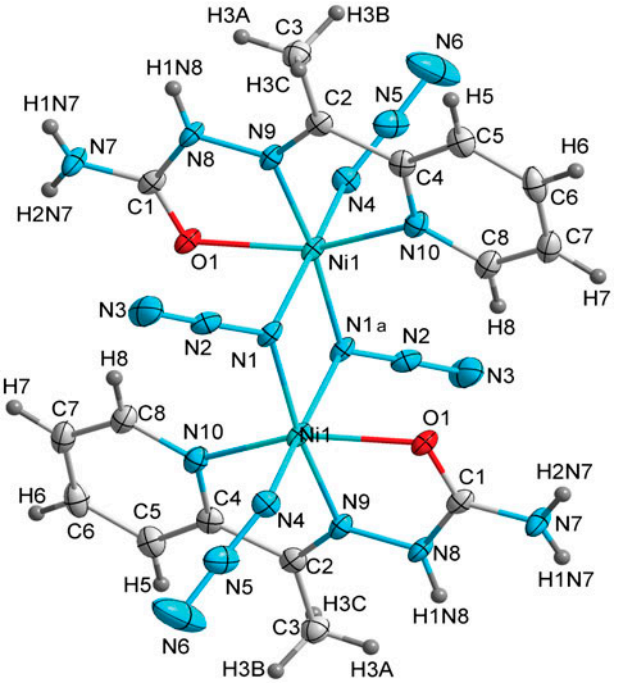

Figure 2. Structure and labeling diagram for $[Ni(HL^1)(N_3)(\mu_{1,1}N_3)]_2$ (**1**).

Table 3. Selected bond lengths (Å) and angles (°) for **1** (experimental data belong to the solid phase, whereas the calculated data correspond to the isolated molecule in a gas phase).

Bond lengths (Å)			Bond angles (°)		
	Experimental	Calculated		Experimental	Calculated
Ni1–Ni1	3.186(6)	2.9815			
Ni1–N1	2.0555(14)	1.9113	N9–Ni1–N1	172.92(6)	15.0991
Ni1–N1a	2.1288(14)	1.9227	N9–Ni1–N4	93.19(6)	87.0649
Ni1–N4	2.0695(14)	1.9033	N9–Ni1–N10	78.45(6)	77.5724
Ni1–N9	1.9952(14)	1.8921	N9–Ni1–O1	78.06(5)	72.7743
Ni1–N10	2.0700(15)	2.3796	N1–Ni1–N4	91.14(6)	92.0723
Ni1–O1	2.1034(12)	2.2316	N1–Ni1–O1	96.51(5)	88.2234
N1–N2	1.209(2)	1.2501	N1–Ni1–N1	80.84(6)	79.6191
N2–N3	1.149(2)	1.1434	N4–Ni–N1	169.56(6)	175.3289
N4–N5	1.191(2)	1.2178	N3–N2–N1	178.65(19)	169.0727
N5–N6	1.150(2)	1.1497	N6–N5–N4	178.3(2)	171.7268

Selected bond parameters observed in **1** are listed in table 3. The Ni–N_{azido}–Ni–N_{azido} rings are planar and the Ni1–N_{azido}–Ni1 bond angle is 99.16(6)°, which falls in the range of published Ni–azide–Ni angles in similar compounds [41, 47–51]. The end-on azide bridges are essentially linear with angles N1–N2–N3 178.65(19)° and show asymmetric N–N distances of 1.209(2)/1.149(2) Å. The terminal azides are quasi-linear with N4–N5–N6 of 178.3(2)° and show asymmetric N–N distances of 1.191(2)/ 1.150(2) Å. The terminal azides are

coordinated *trans* to each other and the N4–Ni1···Ni1–N4 torsion angle is 180°. Two neighboring bridged Ni^{2+} ions give a binuclear unit in which the bond lengths of Ni1–N1 are 2.0555(14) and 2.1288(14) Å. The Ni1···Ni1 separation in the dimer is 3.186(6) Å. These values lie in the typical range for double EO azido-bridging nickel(II) complexes (3.155–3.449 Å) [47–52] (For more information see table 4). The nitrogens of the semicarbazone and azido ligands are involved in intermolecular H-bonding interaction with adjacent dinuclear units. The hydrogen bonds N1···H1–N7 (N1···H1 distance 2.291 Å, N1H1N7 angle 154.81°) and N4···H1–N8 (N1···H1 distance 2.026 Å, N1H1N7 angle is 164.01°) expand the structure of **1** in 2-D.

3.3.2. Structure of [Ni(L^2)(N3)] (2). Complex **2** crystallizes in the monoclinic system with space group $P2_1/n$. The molecular structure and atom numbering scheme of **2** are depicted in figure 3. The crystal data and structure refinement are summarized in table 1. Single X-ray crystal analysis reveals a mononuclear complex with coordination number four for **2**.

Table 4. Structural properties of **1** and selected di-$\mu_{1,1}$ azide bridged nickel(II) complexes.

Complex	Ni–N–Ni (°)	Ni···Ni (Å)	Ni–N(bridging) (Å)	Ref.
$[Ni_2(pbdiim)_4(\mu\text{-}_{1,1}\text{-}N_3)_2]\cdot 2(N_3)\cdot 6(H_2O)$	102.96(13)	3.345(3)	2.138(2), 2.138(2)	[27]
$[M_2(biq)_2(\mu_{1,1}\text{-}N_3)_2Cl_2]$	104.86(17)	3.241(1)	2.028(3), 2.060(4)	[46]
$[M_2(dmbpy)_2(\mu_{1,1}\text{-}N_3)_2(N_3)_2]$	105.1(3)	3.276(2)	2.068(7), 2.060(6)	[46]
$[Ni_2(biq)_2(\mu_{1,1}\text{-}N_3)_2(N_3)_2]$	105.20(8)	3.294(1)	2.068(1), 2.078(2)	[46]
$[Ni_2(L^1)(N_3)_4]$	98.36(2), 97.66(3)	3.155(2)	2.061, 2.108, 2.13, 2.061	[46]
$[Ni_2(L^2)(N_3)_4]\cdot CH_3CN$	101.7(2)	3.329(1)	2.150(6), 2.144(6)	[49]
$[Ni_2(L^3)_2(\mu_{1,1}\text{-}N_3)_2(N_3)_2]$	99.7(4)	3.191(4)	2.086(8), 2.088(9)	[50]
$[Ni2(L^4)_2(\mu_{1,1}\text{-}N_3)_2(N_3)_2]$	100.0(10)	3.222(3)	2.085(2), 2.184(2)	[50]
$[Ni(HL)(\mu_{1,1}N_3)(N_3)]_2$	99.16(6)	3.186(6)	2.1288(14), 2.0555(14)	Present work

Notes: [pbdiim: 2-(2′-pyridyl)benzo[1,2-d:4,5-d′]diimidazole], [biq: 2,2′-biquinoline], [dmbpy: 6,6′-dimethyl-2,2′-bipyridine], (L^1 Schiff base ligand made from the reaction of 2 M of 2-benzoyl pyridine and 1 M of triethylenetetramine), [L^2: prepared from the reaction of 2-benzoylpyridine with N,N0-bis-(3-aminopropyl) ethylenediamine in the 2 : 1 M ratio], [L^3: N,N-bis(2-pyridylmethyl) amine], [L^4: N-(2-pyridylmethyl)-N0,N0-diethylethylenediamine].

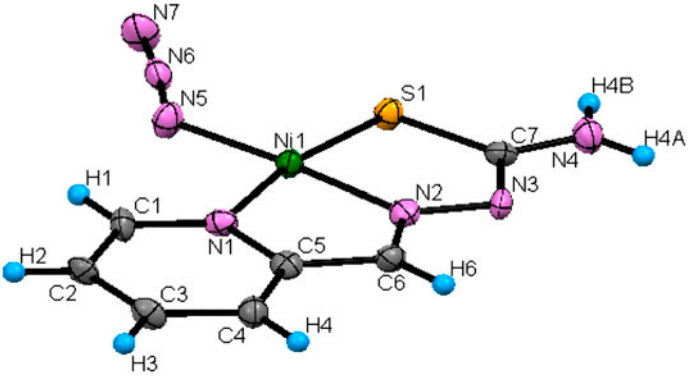

Figure 3. Structure and labeling diagram for [Ni(L^2)(N_3)] (**2**).

The mononuclear unit consists of a Schiff base ligand and a terminal azide. The coordination geometry of Ni(II) is square planar with Ni(II) in the plane made by a pyridyl nitrogen (N1), an azomethine nitrogen (N2), and thioamide sulfur S(1) of the thiosemicarbazone ligand and a nitrogen from azide (N5). Ni(II) ion is 0.038 Å from the average plane formed by N1N2S1N5 in the complex. HL is a tridentate ligand with NNS donors and is deprotonated. It coordinates to Ni(II) in thiol form, also confirmed by the IR spectral data. By considering the bond lengths around Ni(II), Ni1–N1; 1.937(4) Å, Ni1–N2; 1.857(4) Å, Ni1–N5; 1.887(4) Å (for more information about the bond lengths and angles see table 5), similar and in the range 1.857–1.937 Å. The Ni1–S1 (2.1526(14) Å) bond length is longer than the Ni–N bonds, in agreement with those previously reported [11–13]. The C(7)–S(1) bond length in the complex is 1.757(4) Å, similar to those found in related thiosemicarbazone complexes in the thiol form in the solid state, such as 1.76(1) Å in [Ni(dmtsc)] and 1.715(4) Å in [Ni(atsc)]·0.5EtOH] where Hatsc is pyridyl methyl ketone thiosemicarbazone and H2dmtsc is 2,6-diacetylpyridine bis(4N-morpholyl thiosemicarbazone)] [11], 1.74(1) Å in [Cu(NCS)(L)] [where HL is pyridine-2-carbaldehyde thiosemicarbazone[[12], and 1.735(4) Å in [MnL_2[·H_2O [where HL is pyridine-2-carbaldehyde N(4)-p-methoxyphenyl thiosemicarbazone] [13]. The chelate bite angles in the two five-membered rings are also close [N1–Ni1–N2; 83.66(16)° and N2–Ni1–S1; 86.37(12)°]. The terminal azide shows asymmetric N–N distances of 1.209(5)/1.154(5) Å and the azide is quasi-linear with N5–N6–N7; 173.9(4)°. The Ni–N_{azide} distance is 1.887(4) Å for Ni–N(5), similar with those reported for similar structures in the literature [11, 41]. The nitrogen groups of the thiosemicarbazone and azide are involved in intermolecular H-bonds with the adjacent units (for more information see table 6). The N4–H4A···N3 and N4–H4B···N7 are two H-bonds which expand the structure in two directions (see figure 4). Also, the presence of a C–H···S link between C(3) and S(1) is also remarkable. In the complex, the H···S distances is 2.909 Å and the C3H3···S1 angle is

Table 5. Selected bond lengths (Å) and angles (°) for **2** (experimental data belong to the solid phase, whereas the calculated data correspond to the isolated molecule in a gas-phase).

Bond lengths (Å)			Bond angles (°)		
	Experimental	Calculated		Experimental	Calculated
Ni1–N1	1.937(4)	1.9358	N2–Ni1–N5	176.35(16)	176.3527
Ni1–N2	1.857(4)	1.8562	N2–Ni1–N1	83.66(16)	83.6972
Ni1–S1	2.1526(14)	2.1526	N5–Ni1–N1	92.94(16)	92.9194
Ni1–N5	1.887(4)	1.8863	N2–Ni1–S1	86.37(12)	86.3858
S1–C7	1.757(4)	1.7587	N5–Ni1–S1	96.95(12)	96.9257
N3–N2	1.371(5)	1.3711	N1–Ni1–S1	169.67(12)	169.7156
N6–N5	1.209(5)	1.2101	C7–S1–Ni1	95.93(15)	95.9072
N7–N6	1.154(5)	1.1531	N3–N2–Ni1	125.0(3)	124.9698
N3–C7	1.330(6)	1.3287	N6–N5–Ni1	126.9(3)	127.0120
N2–C6	1.315(6)	1.3143	N7–N6–N5	173.9(4)	174.0745
N4–H4A	0.8600	0.8595			
N4–H4B	0.8600	0.8612			

Table 6. Selected hydrogen bonding parameters in **2**.

D–H···A	D–H (Å)	H···A (Å)	D···A (Å)	D–H···A (°)
N4–H4A···N3	0.860	2.119	2.960	165.68
N4–H4B···N7	0.861	2.632	3.230	127.59

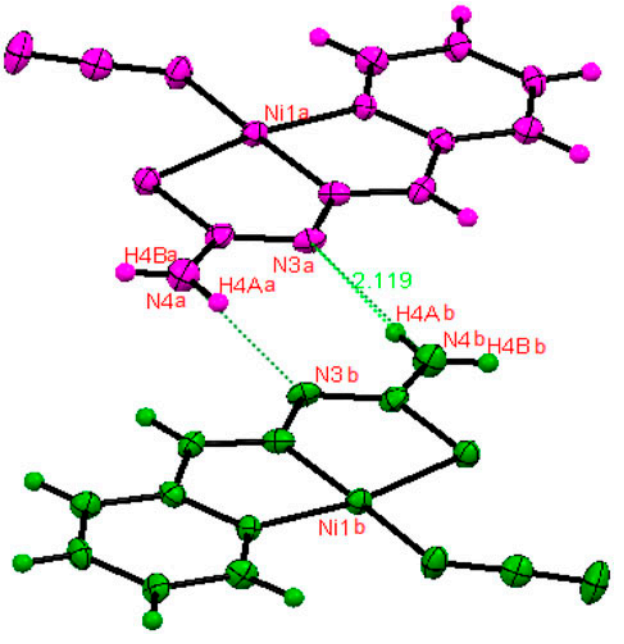

Figure 4. View of presence of N4–H4A···N3 intermolecular H-bonds in **2**.

131.39°; the values suggest strong interactions within this class of weak noncovalent contacts (figure 5). A search for $\pi\cdots\pi$ stacking interactions in the complex revealed that interplanar distance between HL rings is 3.853 Å, similar to the separation of 3.738(3) Å in [MnL_2[·H_2O [with HL pyridine-2-carbaldehyde N(4)-p-methoxy phenyl thiosemicarbazone] [13]. Parallel arrays of the planes of the aromatic moieties in the complex indicate that these interactions are of the slipped face-to-face stacking types. The interplanar distance of 3.853 Å between

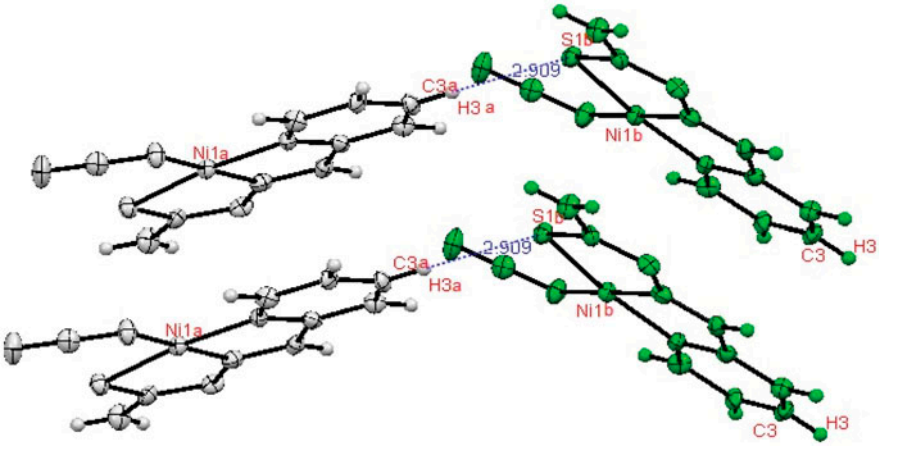

Figure 5. View of presence of the C–H···S linkage between the C(3) and S(1) atoms in **2**.

aromatic rings in the complex is normal for $\pi\cdots\pi$ stacking interactions [53–55]. Also there is a strong C–H$\cdots\pi$ stacking interaction C3–H3$\cdots\pi$, with a separation of 3.531 Å between the hydrogen of the pyridyl ring with the pyridyl ring of the adjacent unit.

3.4. *Antimicrobial screening*

The ligands, **1**, and **2** were tested for their effect on certain bacteria and fungi, and the results are given in table 7. MIC values reveal that HL^1 has weak biological activity but HL^2 with the sulfur donor has better results. The complexes showed enhanced antimicrobial activities against bacteria and fungi than free ligands. The increased activity of the metal chelates can be explained on the basis of chelation theory [1, 8, 11–14, 56–58] and blocking the metal binding sites on enzymes of micro-organisms [56–60]. Comparing MIC values for complexes reveal that **2** has better results than **1**, in agreement with the results of previous research that thiosemicarbazone complexes have better antimicrobial activity than semicarbazone complexes [11–16].

3.5. *DFT calculations*

The structural parameters calculated by the DFT method are listed in tables 3 and 5. The experimental data belong to the solid phase, whereas the calculated data correspond to the isolated molecule in a gas-phase, the parameters only slightly differ from each other. As a result, the calculated geometrical parameters represent a good approximation. The computed IR frequencies are listed in table 8 together with the experimentally determined frequencies. Both calculated and experimental frequencies are in agreement. Also, the value of the energy separation between the highest occupied molecular orbital (HOMO) and the lowest unoccupied molecular orbital (LUMO) was calculated. Figure 6(a) and (b) show the HOMO and LUMO for **1** and **2**, respectively. The HOMO–LUMO energy gap could be regarded as the quantitative index in evaluating the sensitivity of energetic complexes with similar geometric structure. The lower the energy gap, the more sensitive the energetic complex is. The energy gap of **1** and **2** with azido ligands are 2.65 and 3.49 eV. These are in agreement with the fact that the metallic azide is widely used as initiator due to its high sensitivity [61, 62]. Judged

Table 7. The antimicrobial activity of HL^1, HL^2, **1**, and **2** (MIC in $\mu g\,mL^{-1}$).

Compound	*Bacillus subtilis*	*Staphylococcus aureus*	*Escherichia coli*	*Erwinia carotovora*	*Candida kefyr*	*Candida krusei*	*Aspergillus niger*
HL^1	625	1250	1250	1250	625	625	1250
HL^2	312	625	625	312	312	312	625
1	625	625	625	625	625	625	1250
2	154	154	312	312	312	312	312
*Gentamicin	4	8	8	8	–	–	–
*Amphotricin B	–	–	–	–	4	4	16
DMSO	–	–	–	–	–	–	–

*Gentamicin is used as the standard. MIC ($\mu g\,mL^{-1}$) minimum inhibitory concentration, i.e. the lowest concentration to completely inhibit the bacterial growth.
*Amphotricin B is used as the standard. MIC ($\mu g\,mL^{-1}$) minimum inhibitory concentration, i.e. the lowest concentration to completely inhibit the fungal growth.

Table 8. Experimental FT-IR (cm^{-1}) data for **1** and **2** with the theoretical IR (cm^{-1}) data obtained from DFT calculations.

Compound	ν_{NH2}	ν_{NH}	$\nu_{C=O}$ or $\nu_{C=S}$	$\nu_{C=N}$	ν_{N-N}	ν_{N3}
1						
Experimental	3412	3162	1666	1591	1189	2061
Calculated	3532	3574	1709	1586	1207	2080
2						
Experimental	3411	–	809	1638	1168	2052
Calculated	3760	–	722	1613	1055	2027

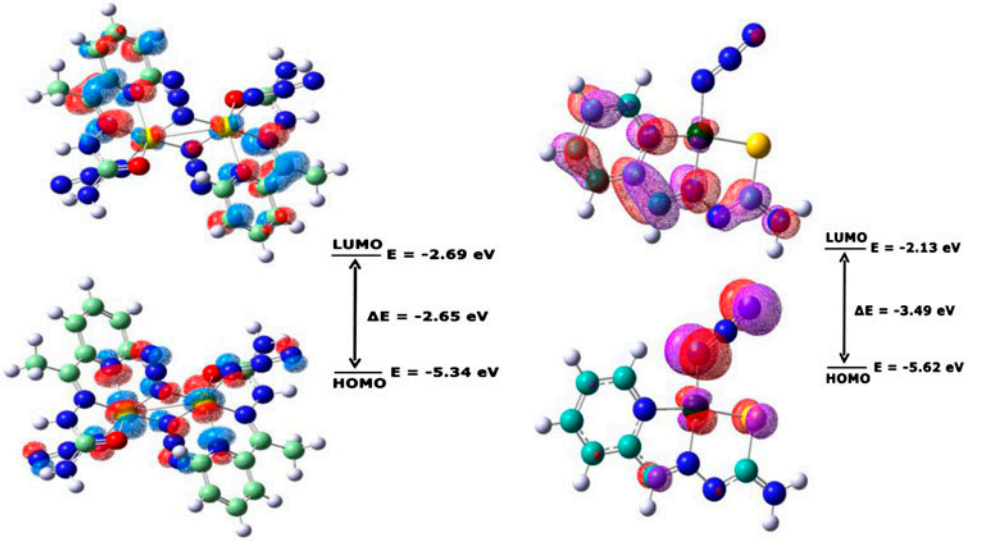

Figure 6. Frontier molecular orbitals for **1** (a) and **2** (b).

by the difference of 0.84 of energy gap between **1** and **2**, **1** is a more sensitive explosive than **2**.

4. Conclusion

Two new complexes of nickel(II), $[Ni(HL^1)(N_3)(\mu_{1,1}N_3)]_2$ (**1**) and $[Ni(L^2)(N_3)]$ (**2**), have been synthesized by slow diffusion in an H-shaped tube. Comparison of the IR spectra of HL^1 and **1** indicates HL^1 is a neutral ligand, chelated to nickel(II) in keto form; for HL^2 and **2**, HL^2 is deprotonated and chelated to the nickel(II) centers in thiol form. Calculated structural parameters and IR spectra for **1** and **2** are in agreement with the crystal structure. Complexes **1** and **2** were structurally characterized by single-crystal X-ray diffraction and the results indicate dinuclear units bridged with azide for **1** and mononuclear **2**. In **1**, each Ni(II) in the dinickel core is further bound by tridentate HL^1, two bridging azides and a terminal azide. Both nickel centers have distorted octahedral geometry. For mononuclear **2**, Ni (II) is bound by tridentate HL^2 and a terminal azide with square-planar geometry.

Antimicrobial activities demonstrate that HL^2 has better results than HL^1 and **2** has better antimicrobial activities than **1** due to sulfur donors of thiosemicarbazone. The DFT calculations for **1** and **2** demonstrate that both calculated and experimental frequencies are in agreement. Judged by 0.84 energy gap between **1** and **2**, **1** would be a more sensitive explosive than **2**.

Supplementary material

Crystallographic data (excluding structure factors) for all the structures reported in this paper have been deposited with the Cambridge Crystallographic Data Center as supplementary publication Nos. CCDC 901690 and 889344 for **1** and **2**. Copies of these data can be obtained free of charge on application to CCDC, 12 Union Road, Cambridge CB2 2EZ, UK; Fax: (+44) 1223 336033, or online via www.ccdc.cam.ac.uk/data_request/cif or by emailing data_request@ccdc.cam.ac.uk.

Acknowledgements

We are grateful to Tabriz University of Research council for the financial support of this research. We also acknowledge the project Praemium Academiae of the Academy of Sciences of the Czech Republic. We are thankful to Departamento de Química Fundamental, Universidade da Coruña of Spain and Department of Chemistry, Indian Institute of Technology Kanpur, for kindly helping.

References

[1] G.G. Mohamed, M.A. Zayed, S.M. Abdallah. *J. Mol. Struct.*, **979**, 62 (2010).
[2] C. Maxim, T.D. Pasatoiu, V.Ch. Kravtsov, S. Shova, C.A. Muryn, R.E.P. Winpenny, F. Tuna, M. Andruh. *Inorg. Chim. Acta*, **361**, 3903 (2008).
[3] S. Nayak, P. Gamez, B. Kozlevc˘ar, A. Pevec, O. Roubeau, S. Dehnen, J. Reedijk. *Polyhedron*, **29**, 2291 (2010).
[4] G.G. Mohamed, M.M. Omar, A.A. Ibrahim. *Spectrochim. Acta Part A*, **75**, 678 (2010).
[5] S. Meghdadi, M. Amirnasr, K. Mereiter, H. Molaee, A. Amiri. *Polyhedron*, **30**, 1651 (2011).
[6] S. Baluja, A. Solanki, N. Kachhadia. *J. Iran. Chem. Soc.*, **3**, 312 (2006).
[7] T. Rosu, E. Pahontu, C. Maxim, R. Georgescu, N. Stanica, G.L. Almajan, A. Gulea. *Polyhedron*, **29**, 757 (2010).
[8] N. Raman, S. Sobha, A. Thamaraichelvan. *Spectrochim. Acta Part A*, **78**, 888 (2011).
[9] J.G. Tojal, J.L. Pizarro, A. García-Orad, A.R. Pérez-Sanz, M. Ugalde, A.A. Díaz, J.L. Serra, M.I. Arriortua, T. Rojod. *J. Inorg. Biochem.*, **86**, 627 (2001).
[10] E. Viñuelas-Zahínos, F. Luna-Giles, P. Torres-García, M.C. Fernández-Calderón. *Eur. J. Med. Chem.*, **46**, 150 (2011).
[11] N.Ch. Kasuga, K. Sekino, Ch. Koumo, N. Shimada, M. Ishikawa, K. Nomiya. *J. Inorg. Biochem.*, **84**, 55 (2001).
[12] N.Ch. Kasuga, K. Sekino, M. Ishikawa, A. Honda, M. Yokoyama, S. Nakano, N. Shimada, Ch. Koumo, K. Nomiya. *J. Inorg. Biochem.*, **96**, 298 (2003).
[13] N.Ch. Kasuga, K. Onodera, S. Nakano, K. Hayashi, K. Nomiya. *J. Inorg. Biochem.*, **100**, 1176 (2006).
[14] B. Shaabani, A.A. Khandar, F. Mahmoudi, M.A. Maestro, L. Cunha-Silva, S.S. Balula. *Polyhedron*, **57**, 118 (2013).
[15] J. Garcia-Tojal, L. Lezama, J.L. Pizarro, M. Insausti, M.I. Arriortu, T. Rojo. *Polyhedron*, **18**, 3703 (1999).
[16] H. Elo. *Z. Naturforsch.*, **62c**, 498 (2007).
[17] A. Karakucuk-Iyidogan, D. Tasdemir, E.E. Oruc-Emre, J. Balzarini. *Eur. J. Med. Chem.*, **46**, 5616 (2011).

[18] S. Chandra, A. Kumar. *Spectrochim. Acta Part A*, **68**, 1410 (2007).
[19] V.M. Leovac, L. Bjelica, L. Jovanovic. *Polyhedron*, **4**, 233 (1985).
[20] T.A. Reena, E.B. Seena, M.R. Prathapachandra Kurup. *Polyhedron*, **27**, 1825 (2008).
[21] B.-L. Liu, H.-P. Xiao, E.N. Nfor, Y. Song, X.-Z. You. *Inorg. Chem. Commun.*, **12**, 8 (2009).
[22] A. Ray, G.M. Rosair, G. Pilet, B. Dede, C.J. Gómez-García, S. Signorella, S. Bellú, S. Mitra. *Inorg. Chim. Acta*, **375**, 20 (2011).
[23] A.M. Madalan, M. Noltemeyer, M. Neculai, H.W. Roesky, M. Schmidtmann, A. Müller, Y. Journaux, M. Andruh. *Inorg. Chim. Acta*, **359**, 459 (2006).
[24] Ch. Adhikary, D. Mal, K.-I. Okamoto, S. Chaudhuri, S. Koner. *Polyhedron*, **25**, 2191 (2006).
[25] W.-W. Sun, X.-B. Qian, Ch.-Y. Tian, E.-Q. Gao. *Inorg. Chim. Acta*, **362**, 2744 (2009).
[26] F.A. Mautner, A. Egger, B. Sodin, M.A.S. Goher, M.A.M. Abu-Youssef, A. Massoud, A. Escuer, R. Vicente. *J. Mol. Struct.*, **969**, 192 (2010).
[27] S. Shit, P. Talukder, J. Chakraborty, G. Pilet, M.S. El Fallah, J. Ribas, S. Mitra. *Polyhedron*, **26**, 1357 (2007).
[28] X.-L. Yu, W.-S. You, X. Guo, L.-C. Zhang, Y. Xu, Z.-G. Sun, R. Clérac. *Inorg. Chem. Commun.*, **10**, 1335 (2007).
[29] A. Ray, G.M. Rosair, G. Pilet, B. Dede, C.J. Gómez-García, S. Signorella, S. Bellú, S. Mitra. *Inorg. Chim. Acta*, **375**, 20 (2011).
[30] A. Dehno Khalaji, H. Stoekli-Evans. *Polyhedron*, **28**, 3769 (2009).
[31] A.A. Soudi, A.H. White. *Aust. J. Chem.*, **49**, 1029 (1996).
[32] F. Marandi, B. Mirtamizdoust, A.A. Soudi, H.-K. Fun. *Inorg. Chem. Commun.*, **10**, 174 (2007).
[33] G. Mahmoudi, A. Morsali. *Inorg. Chim. Acta*, **362**, 3238 (2009).
[34] B. Shaabani, A.A. Khandar, M. Dusek, M. Pojarova, F. Mahmoudi. *Inorg. Chim. Acta*, **394**, 563 (2013).
[35] Agilent. *CrysAlis PRO*, Agilent Technologies UK Ltd, Yarnton (2010).
[36] A.D. Becke. *J. Chem. Phys.*, **98**, 5648 (1993).
[37] C. Lee, W. Yang, R.G. Parr. *Phys. Rev. B*, **37**, 785 (1988).
[38] P.J. Hay, W.R. Wadt. *J. Chem. Phys.*, **82**, 270 (1985).
[39] A description of the basis sets and theory level used in this work can be found in the following: J.B. Foresman, A.E. Frisch. *Exploring Chemistry with Electronic Structure Methods*, 2nd Edn, Gaussian Inc., Pittsburgh, PA (1996).
[40] M.J. Frisch, G.W. Trucks, H.B. Schlegel, G.E. Scuseria, M.A. Roob, *GAUSSIAN 98, Revision A.9*, Gaussian Inc., Pittsburgh, PA (1998).
[41] S. Deoghoria, S. Sain, M. Soler, W.T. Wong, G. Christou, S.K. Bera, S.K. Chandra. *Polyhedron*, **22**, 261 (2003).
[42] V. Philip, V. Suni, M.R. Prathapachandra Kurup, M. Nethaji. *Polyhedron*, **23**, 1225 (2004).
[43] B. Machura, A. Switlicka, I. Nawrot, J. Mrozin ski, K. Michalik. *Polyhedron*, **30**, 2815 (2011).
[44] P. Mukherjee, O. Sengupta, M.G.B. Drew, A. Ghosh. *Inorg. Chim. Acta*, **362**, 3285 (2009).
[45] Zh.-H Zhang, X.-H. Bu, Zh.-H. Ma, W.-M. Bu, Y. Tang, Q.-H. Zhao. *Polyhedron*, **19**, 1559 (2000).
[46] P. Chaudhuri, T. Weyhermtiller, E. Bill, K. Wieghardt. *Inorg. Chim. Acta*, **252**, 196 (1996).
[47] X.-J. Lin, Zh. Shen, Y. Song, H.-J. Xu, Y.-Zh. Li, X.-Z. You. *Inorg. Chim. Acta*, **358**, 1963 (2005).
[48] H.-Zh. Kou, Sh. Hishiya, O. Sato. *Inorg. Chim. Acta*, **361**, 2396 (2008).
[49] S. Sain, S. Bid, A. Usman, H.-K. Fun, G. Aromí, X. Solans, S.K. Chandra. *Inorg. Chim. Acta*, **358**, 3364 (2005).
[50] S. Sarkar, A. Mondal, A. Banerjee, D. Chopra, J. Ribas, K.K. Rajak. *Polyhedron*, **25**, 2285 (2006).
[51] S. Sarkar, A. Mondal, M.S. El Fallah, J. Ribas, D. Chopra, H. Stoeckli-Evans, K.K. Rajak. *Polyhedron*, **25**, 28 (2006).
[52] P.T. Kissinger, W.R. Heineman. *J. Chem. Educ.*, **60**, 702 (1983).
[53] F. Marandi, P. McArdle, B. Mirtamizdoust, A.A. Soudi. *J. Coord. Chem.*, **60**, 891 (2007).
[54] C.A. Hunter, J.K.M. Sanders. *J. Am. Chem. Soc.*, **112**, 5525 (1990).
[55] J.C. Collings, K.P. Roscoe, E.G. Robins, A.S. Batsanov, L.M. Stimson, J.A.K. Howard, S.J. Clark, T.B. Marder. *New J. Chem.*, **26**, 1740 (2002).
[56] N.P. Priya. *Int. J. Appl. Biol. Pharm. Tech.*, **2**, 538 (2011).
[57] A.A. Nejo, G.A. Kolawole, A.O. Nejo. *J. Coord. Chem.*, **63**, 4398 (2010).
[58] L. Mishra, V.K. Singh. *Indian J. Chem.*, **32A**, 446 (1993).
[59] R.J. Carlin, A.J. van Duyeneveldt. *Magnetic Properties of Transition Metal Compounds*, Springer Verlag, New York (1977).
[60] G. Chastanet, B. Le Guennic, C. Aronica, G. Pilet, D. Luneau, M.-L. Bonnet, V. Robert. *Inorg. Chim. Acta*, **361**, 3847 (2008).
[61] B. Tang, J.-H. Ye, X.-H. Ju. *Int. Scholarly Res. Network ISRN Org. Chem.*, **2011**, 1 (2011).
[62] B. Shaabani, B. Mirtamizdoust, M. Shadman, H.-K. Fun. *Z. Anorg. Allg. Chem.*, **635**, 2642 (2009).